



## Earthquake Hazard Assessment in the Oran Region (Northwest Algeria)

YOUCEF BOUHADAD and NASSER LAOUAMI

*National Center of Applied Research in Earthquake Engineering, C.G.S., 1 rue Kadour Rahim  
H.Dey BP 252, Alger, Algeria*

(Received: 8 December 1999; accepted in revised form: 3 July 2001)

**Abstract.** This paper deals with the probabilistic seismic hazard analysis carried out in the Oran region, situated in the Northwest of Algeria. This part of Algeria was historically struck by strong earthquakes. It was particularly affected during the October 9, 1790 Oran earthquake of intensity X. The main purpose of this work is to assess seismic hazard on rocks in order to provide engineers and planners with a basic tool for seismic risk mitigation. The probabilistic approach is used in order to take into account uncertainties in seismic hazard assessment. Seismic sources are defined in the light of the most recent results obtained from seismotectonics analyses carried out in North Algeria. Source parameters such as *b*-values, slip rate and maximum magnitude are assessed for each seismic source. The attenuation of ground shaking motion with distance is estimated by using attenuation relationships developed elsewhere throughout the world (Sadigh *et al.*, 1993; Ambraseys and Bommer, 1991). The two relationships agree well with the local data. Different choices of source parameter values and attenuation relationships are assigned weights in a logic tree model. Results are presented as relationships between values of peak ground acceleration (PGA) and annual frequency of exceedance, and maps of hazard for return periods of 200 years and 500 years. A maximum peak ground acceleration of 0.42 g is obtained for the Oran site for a return period of 500 years.

**Key words:** probabilistic analysis, Algeria, hazard maps, rocks, seismic source parameters, attenuation law.

### 1. Introduction

The first step in reducing the risk to society from natural disasters is an assessment of the hazard itself. This means that the reduction of earthquake risk, whether it depends on other aspects such as the vulnerability of the exposed population, should be based on the knowledge about the expected level of ground motion that may be experienced in the area within given mean return periods, such as 100, 200 or 500 years. Recent development in the field of seismotectonics, including identification of active faults by using new techniques, such as Digital Elevation Models, as well as in the field of seismicity, particularly the recent homogenisation and completeness analysis of Algerian historical seismicity data, and advances in techniques of seismic hazard assessment throughout the world, make possible the construction of seismic hazard maps in term of maximum peak ground acceleration.

This should serve as a basic element of strategies of development of the region under consideration. In Algeria, earthquake hazard constitutes a constant threat to human lives and properties. The rapid urbanisation, growth of old cities, appearance of highly vulnerable new urban sites, and the concentration of populations in hazardous areas, contribute to heavy loss of human lives and increase the cost of damage in the case of an earthquake. Several strong and destructive earthquakes have occurred in North Algeria with at least 50,000 recorded deaths (CRAAG, 1994). For the Oran region, situated in the Northwest of Algeria, seismic hazard assessment should be the basic step in each strategy dealing with seismic risk mitigation. This suggestion is due to the fact that the Oran region and its vicinity is an area prone to destructive, moderate to strong earthquakes. Indeed, the region experienced several major destructive seismic events in the past, particularly the Oran October 9, 1790 earthquake of intensity X (MSK scale), which caused about 3,000 deaths, and the Beni-Chougrane earthquake of August 18, 1994 of intensity VIII ( $M_s = 5.6$ ), where 171 human lives were claimed and about 1000 houses, mainly rural non engineered constructions, collapsed (CGS, 1995).

The region under consideration is caught between the African and Eurasian tectonic plates, which have been converging along a N-S to NNW-SSE direction since at least the early Quaternary period. The boundary between these two tectonic plates is very complex and not well defined (McKenzie, 1972; Philip, 1987). As a result of this geodynamic process a large band of about 100–150 km, constituted by deformed quaternary and neogene deposits, appears in the northern part of Algeria namely the Tellian chain (Philip and Thomas, 1977; Philip and Meghraoui, 1983; Thomas, 1985). The rate of motion determined from paleoseismological data (Meghraoui *et al.*, 1988) and from analysis of source mechanisms (De Mets *et al.*, 1990) is about 4–6 mm/y. In detail, the Tellian chain is formed by folds lying NE-SW which are organised in an echelon system. This is likely due to the presence of deep E-W strikes slip (Meghraoui *et al.*, 1996). These folds are often asymmetric and associated with reverse faults (WCC, 1984; Aoudia and Meghraoui, 1995). The recent earthquakes of El Asnam, October 10, 1980 of magnitude  $M_S = 7.3$ , Chenoua October 29, 1989 of magnitude  $M_S = 6.1$  and Mascara August 18, 1994 of magnitude  $M_S = 5.6$ , show how this kind of structure (faulted-folds) could be seismogenic (Yielding *et al.*, 1989; Meghraoui, 1990; Benouar *et al.*, 1994; Bezzeghoud and Bufforn, 1999). Indeed, faulted folds are the main seismogenic geological structures in North Algeria. A relatively high and destructive emergence of seismicity resulted from the tectonic activity during at least the last two centuries. In examining the map of historical seismicity of Algeria for the period of 1365-1992 (Figure 1), it appears that the seismicity is concentrated in areas such as Chellif-Ain Deffa, Algiers-Tipaza, Babor, Constantine-Guelma and the region of Oran-Beni Chougrane, which is the concern of this study. This region is defined by the following longitude-latitude co-ordinates:  $1^{\circ}.10$  W– $0^{\circ}.11$  E and  $36^{\circ}.04$  N– $35^{\circ}.04$  N (Figure 3). This is an area of about  $14570 \text{ km}^2$  within which

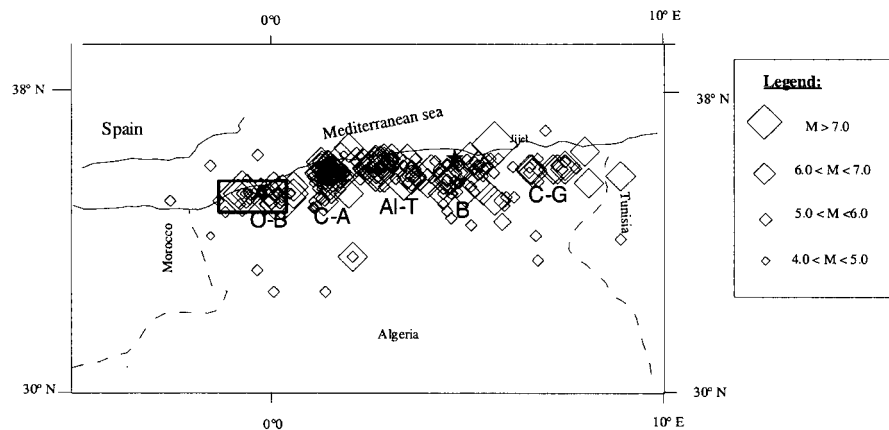


Figure 1. Seismicity map of the Tellian Atlas of Algeria for the period of 1365–1992. Location of epicentres are from historical seismicity catalogues of CRAAG, 1994 and Benouar, 1994. Areas of special concentration of epicentres are indicated by letters: O–B = Oran–Beni–Chougrane, C–A = Chlef–Ain Defla, Al–T = Algiers–Tipaza, B = Babor and C–G = Constantine–Guelma. The rectangle represents the studied area (see Figure 4).

many important cities are located, such as Oran, Mostaganem, Mascara and Sidi Bel Abbas.

This study presents the seismotectonic framework of the region under consideration, the identification of seismic sources and an assessment of their parameters. Furthermore, a local attenuation relationship derived from data recorded during the Beni Chougrane earthquake of August 18, 1994 of Magnitude  $M_s = 5.6$ , is compared to the two world-wide relationships of Ambraseys and Bommer (1991) and Sadigh *et al.* (1993). Probabilistic hazard assessment is performed by using a computer program (Geomatrix, 1993) based on the original algorithm developed by Cornell (1968). Results are presented as relationships between values of horizontal peak ground acceleration (PGA) and annual frequencies of exceedance and maps of horizontal PGA for different return periods.

## 2. Mathematical Formulation of the Probabilistic Seismic Hazard Analysis

The probabilistic approach to seismic hazard analysis, used hereafter, was proposed by Cornell in 1968 and developed in its computer form by McGuire (1976) and Geomatrix (1993). It is assumed that the occurrence of earthquakes in a seismic source results from a Poisson process. Then, the probability that at a given site a ground motion parameter,  $Z$ , will exceed a specified level,  $z$ , during a specified time,  $T$ , is represented by the expression:

$$P(Z > z) = 1.0 - e^{-\nu(z)T} \leq \nu(z)T, \quad (1)$$

where  $\nu(z)$  is the average frequency during time period  $T$  at which the level of ground motion parameter,  $Z$ , exceed level  $z$  at a given site. The function  $\nu(z)$

incorporates the uncertainty in time, size and location of future earthquakes and uncertainty in the level of ground motion they produce at the site. It is given by:

$$\nu(z) = \sum_{n=1}^N N_n(m^0) \int_{m=m^0}^{m^u} f_n(m) \left[ \int_{r=0}^{\infty} f_n(r|m) P(Z > z|m, r) dr \right] dm, \quad (2)$$

where  $N_n(m^0)$  is the frequency of earthquakes on seismic source  $n$  above a minimum magnitude  $m^0$  that is taken equal to 5.0 in this work. Indeed, below this value, magnitudes are considered to be without engineering significance;  $f_n(m)$  is the probability density function for event size between  $m^0$  and a maximum event for the source,  $m^u$ ;  $f_n(r|m)$  is the conditional probability density function for distance to earthquake rupture;  $P(Z > z|m, r)$  is the probability that, given a magnitude  $m$  earthquake at a distance  $r$  from the site, the ground motion exceeds level  $z$ . In practice, the integrals in Equation (2) are replaced by summations and the density functions  $f(m)$  and  $f(r|m)$  are replaced by discrete mass functions. The resulting expression for  $\nu(z)$  is given by

$$\nu(z) = \sum_{n=1}^N \sum_{m_i=m^0}^{m_i=m^u} \lambda_n(m_i) \left[ \sum_{r_j=r_{\min}}^{r_j=r_{\max}} P_n(R = r_j|m_i) P(Z > z|m_i, r_j) \right], \quad (3)$$

where  $\lambda_n(m_i)$  is the frequency of events of magnitude  $m_i$  occurring on source  $n$  obtained by discretizing the earthquake recurrence relationship for source  $n$ . Different choices of source parameters values as well as different attenuation relationships are assigned appropriate weight in the framework of a logic tree model (Figure 2) (NRC, 1988). The weight assigned to different parameters was based on our knowledge of the seismotectonic conditions of the region. Results are shown in terms of mean, median (50th percentile), 15th percentile, and 85th percentile values of annual probability of exceedance versus peak ground acceleration in rock, in order to illustrate the uncertainties involved in seismic hazard calculations (McGuire, 1993; Toro, 1995).

### 3. Seismic Sources Identification

Seismic hazard analysis requires a good definition of the location and geometry of the potential seismic sources. It's assumed that characteristics such as rate of activity within a given source are uniform. Earthquakes occur following relative slippage of two earth blocks along a fault plane; Therefore it's more realistic, firstly, to model seismic sources as line sources representing the faults. In examining the map of the major faults of the region under consideration (Figure 3), it appears that all these faults lie NE–SW, perpendicular to the direction of regional stress. The mapped active faults in the studied region were determined in recent studies, based on geological, geomorphological and geophysical observations (Thomas, 1985;

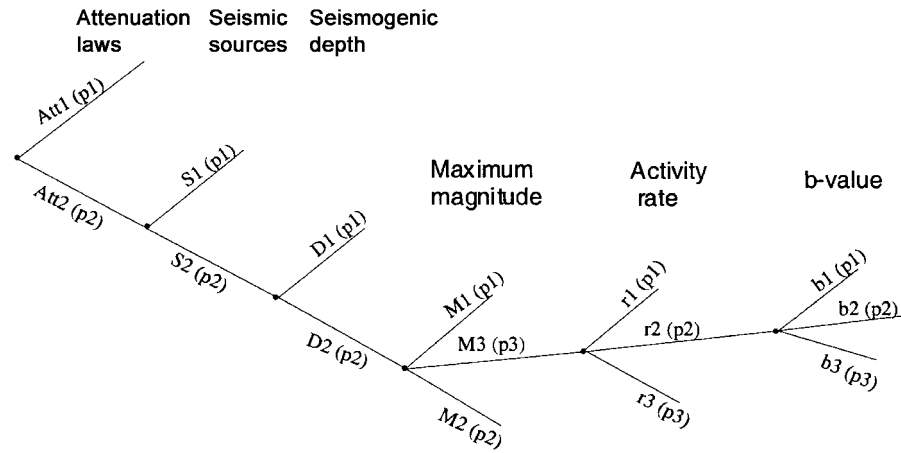


Figure 2. Logic tree model showing a graphical representation of the involved parameters and their associated probabilities.

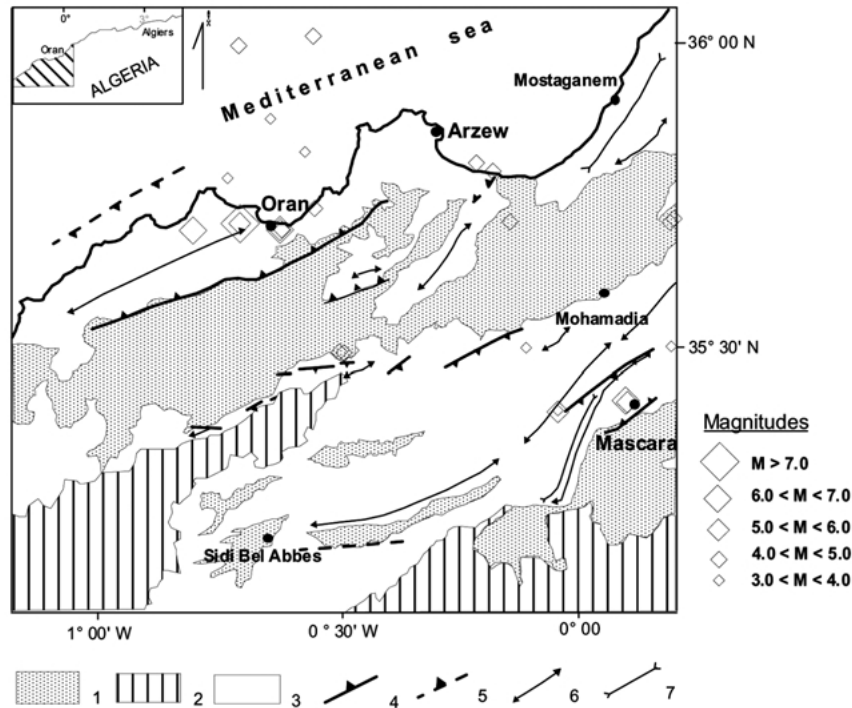


Figure 3. Seismotectonic map of the studied region showing the mainly identified active faults. 1. Quaternary deposits, 2. Anté-neogene deposits, 3. Neogene deposits, 4. Active reverse fault, 5. Interpreted fault, 6. Anticline axis, 7. Syncline axis. The seismicity shown represent the 1365–1992 period (CRAAG, 1994; Benouar, 1994).

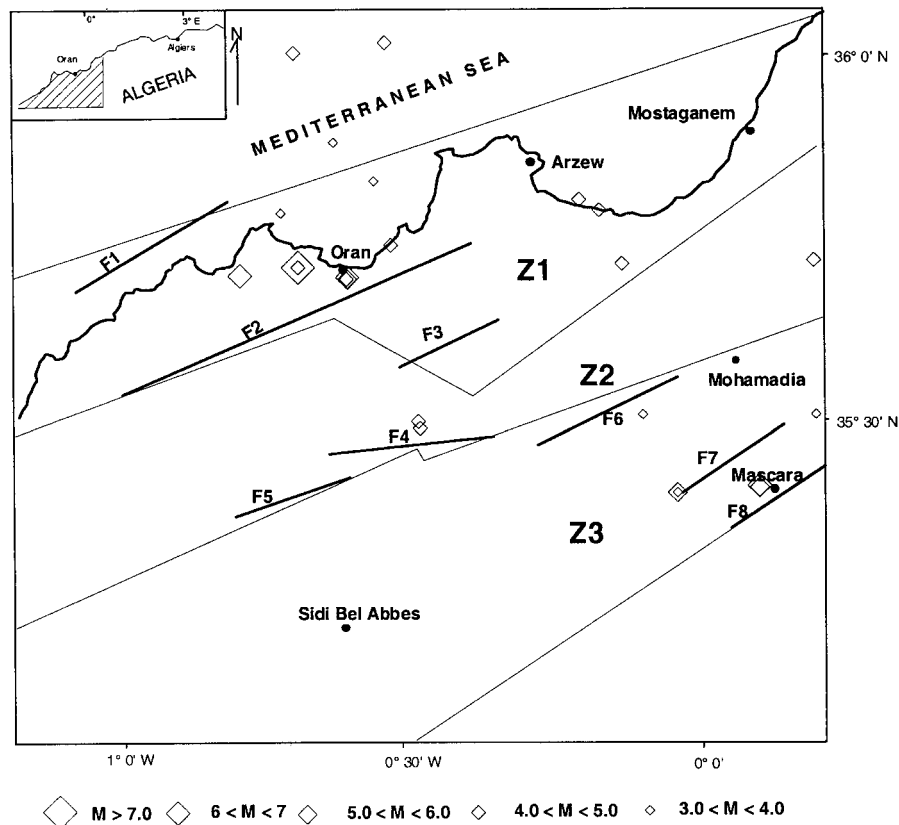


Figure 4. Modelisation of the identified active faults as line sources and the defined seismic zones as areas sources. F1 = Offshore interpreted fault, F2 = Oran fault, F3 = Arzew fault, F4 = South East Mleta fault, F5 = Southwest Mleta fault, F6 = South Habra fault, F7 = Beni-Chougrane fault, F8 = Ghris fault, Z1 = Oran plateau area source, Z2 = Mleta-Habra basins area source, Z3 = Beni-Chougrane area source.

Meghraoui, 1988; Bouhadad, 1997). Concerning the offshore fault (F1 in Figure 4), it's interpreted according to geophysical and bathymetric data (El Ghoibrini, 1986).

Being an interplate region, the active faults in Oran are well identified, and are considered to be the primary cause of earthquakes in this region, as suggested by the good correlation between historical seismicity and geological features. However, three regional seismic area sources are defined on the basis of geological and seismological characteristics in order to take into account the eventually unknown blind faults. These area sources correspond principally to the inter-fault blocks. Earthquakes are considered to occur randomly within the defined area sources. Figure 4 shows the potentially active faults modelled as line sources and the defined seismic source zones modelled as area sources.

#### 4. Seismic Sources Parameters

Tables I and II show respectively the assessed parameters for the mapped active faults and for the defined seismic areas source. The recently homogenised, completed and compiled earthquake catalogues (Benouar, 1994, CRAAG, 1994) were used to assess the seismogenic depth and the parameters of the Gutenberg and Richter (1954) relationship.

The parameter  $b$  is one of the basic parameters in seismic hazard assessment. It's assumed to be connected to the tectonic heterogeneity of the area. The  $b$  parameter is determined for each seismic source by using the regression fits method for the identified faults (Figure 5, Table I), while for the defined seismic area sources the Kijko and Sellevoll (1989) method is used to calculate  $b$ -values and  $N(m^0)$  (Table II). Because of the uncertainties which characterise the location of epicenters and the lack of seismic data, we used (in computing  $b$ -value for seismic sources) all epicenters located in the vicinity of the considered source, generally up to 10 km from the source which seemed to result from its activity. In this way, mislocation of historical epicenters up to 10 km is taken into account (Benouar, 1994). Therefore, the same epicenters used are sometimes associated with more than one seismic source (Figure 6).

Earthquakes in Algeria often occur at a depth of less than 20 km along 40° to 65° dipping reverse faults (Yielding *et al.*, 1989; Meghraoui, 1990; Benouar *et al.*, 1994). In order to take uncertainties in the geometry of faults into account, three values of dip angles are considered (Table I).

The expected maximum magnitudes are assessed by using updated world-wide empirical relationships (Wells and Coppersmith, 1994) that link geometrical characteristics of the fault, such as length and area to the magnitude:

$$M = 5.00 + 1.22 \log (\text{SRL}) \quad (4)$$

$$M = 4.33 + 0.90 \log (\text{RA}), \quad (5)$$

where SRL is the surface rupture length and RA is the rupture area. The standard deviation in Equations (4) and (5) are 0.28 and 0.25, respectively, taken from Wells and Coppersmith (1994).

Lack of local data meant that the available regional paleoseismological data, and interpretation of geomorphic features, such as uplift of marine and alluvial terraces (Merrits and Bull, 1989), are used to assess slip rates of faults .

Some faults such as the Oran fault, Arzew fault, Beni-Chougrane fault and Ghris fault present strong analogies with the Oued Fodda fault (Meghraoui, 1988; Benouar *et al.*, 1994), situated about 200 km east of the studied region, which caused the El Asnam earthquake of October 10, 1980 ( $M_s = 7.3$ ). Trench investigations on the 1980 trace of the Oued Fodda fault provided useful paleoseismic data, which are used herein to estimate slip rate of the above mentioned faults (WCC, 1984; Meghraoui *et al.*, 1988; Swan, 1988). Indeed, according to Meghraoui *et al.* (1988),

*Table 1.* Seismotectonic characteristics of the potentially active faults in the studied region. The number of values for each parameter change from one source to an other depending on the state of our knowledge of the source.

Fault name	Source mechanism	Dip (degree)	Maximum magnitude/ associated weight	<i>b</i> -value/ associated weight	Slip rate (mm/y)/ associated weight
Offshore	Reverse	40°	6.75 (0.7)	0.47 (0.2)	0.30 (0.6)
		55°	7.0 (0.3)	0.30 (0.6)	0.50 (0.4)
		65°		0.13 (0.2)	
Oran	Reverse	40°	7.25 (0.6)	0.47 (0.2)	0.30 (0.15)
		55°	7.5 (0.2)	0.30 (0.6)	0.40 (0.14)
		65°	7.0 (0.2)	0.13 (0.2)	0.50 (0.15)
					0.70 (0.14)
Arzew	Reverse	40°	6.5 (0.5)	0.32 (0.2)	0.30 (0.15)
		55°	6.75 (0.5)	0.30 (0.6)	0.40 (0.4)
		65°		0.28 (0.2)	0.50 (0.15)
					0.65 (0.3)
Mleta East	Reverse	40°	7.0 (0.5)	0.29 (0.2)	0.30 (0.2)
		55°	6.75 (0.5)	0.27 (0.6)	0.50 (0.3)
		65°		0.25 (0.2)	0.15 (0.50)
Mleta West	Reverse	40°	6.5 (0.5)	0.29 (0.2)	0.30 (0.2)
		55°	6.75 (0.5)	0.27 (0.6)	0.50 (0.3)
		65°		0.25 (0.2)	0.15 (0.50)
Beni-Chougrane	Reverse	40°	7.0 (0.5)	0.34 (0.2)	1.40 (0.42)
		55°	6.75 (0.25)	0.24 (0.6)	0.70 (0.14)
		65°	6.50 (0.25)	0.14 (0.2)	0.50 (0.34)
Ghris	Reverse	40°	6.50 (0.5)	0.34 (0.2)	0.30 (0.3)
		55°	6.75 (0.5)	0.24 (0.6)	0.50 (0.3)
		65°		0.14 (0.2)	1.40 (0.3)
					0.70 (0.1)
Habra	Reverse	40°	7.0 (0.5)	0.29 (0.2)	0.30 (0.2)
		55°	6.75 (0.5)	0.27 (0.6)	0.50 (0.6)
		65°		0.25 (0.2)	0.70 (0.1)
					0.30 (0.1)



Table II. Seismotectonic characteristics of the defined seismic area source in the studied region.

Area source name	Maximum magnitude/associated weight	<i>b</i> -values/associated weight	<i>N</i> ( <i>m</i> <sub>0</sub> )/associated weight
Oran plateau seismic area source (Z1)	7.25 (0.2)	0.31 (0.2)	0.50 (0.6)
	7.0 (0.6)	0.43 (0.6)	0.60 (0.4)
	6.50 (0.2)	0.55 (0.2)	
Habra-Mleta quaternary basins seismic area source (Z2)	5.50 (0.2)	0.36 (0.2)	0.65 (0.6)
	6.0 (0.6)	0.47 (0.6)	0.35 (0.4)
	6.50 (0.2)	0.58 (0.2)	
Beni-Chougrane seismic area source (Z3)	7.0 (0.2)	0.10 (0.2)	0.12 (0.4)
	6.75 (0.6)	0.27 (0.6)	0.18 (0.6)
	6.50 (0.2)	0.45 (0.2)	

based on trench investigations, the slip rate along the Oued Fodda fault ranges from 0.65–2.35 mm/y.

Also, we consider in this study, based on the impressive recent tectonic deformation observed in the studied region (Figure 3), that the Oran fault, which is the most important geological structure in the region, may absorb at least 1/3 of the regional shortening rate estimated at 4–6 mm/y, that is why we attributed a slip rate of 1.8 mm/y as a possible alternative for the Oran fault (Table I). On the other hand, uniform uplift rates (Merritts and Bull, 1989) obtained by using marine and alluvial terraces mapped in the studied region at different elevations, are converted to slip rate by considering different dips of faults. The obtained values of slip rate for different faults ranges from 0.15–0.50 mm/y (Table I).

The magnitude recurrence model for a seismic source specifies the frequency of seismic events of various sizes per year. It's determined from historical seismicity and geological data. Two models are used in this work: The truncated exponential recurrence model (Cornell and Van Marke, 1969) for seismic source areas, given by the following expression:

$$N(m) = N(m_0) \frac{e^{-\beta(m-m^0)} - e^{-\beta(m^u-m^0)}}{1.0 - e^{-\beta(m^u-m^0)}} \text{ for } m^0 \leq m < m^u, \quad (6)$$

where  $\beta = b \ln(10)$  and  $m^u$  is the maximum magnitude, and the characteristic size recurrence model (Youngs and Coppersmith, 1985) for a specific fault, given by the following expression:

$$N(m) = N^e \frac{e^{-\beta(m-m^0)} - e^{-\beta(m^1-m^0)}}{1.0 - e^{-\beta(m^1-m^0)}} + N^c \text{ for } m^0 \leq m < m^1$$

$$N(m) = N^c \frac{m^u - m}{m^u - m_1} \text{ for } m^1 \leq m < m^u, \quad (7)$$

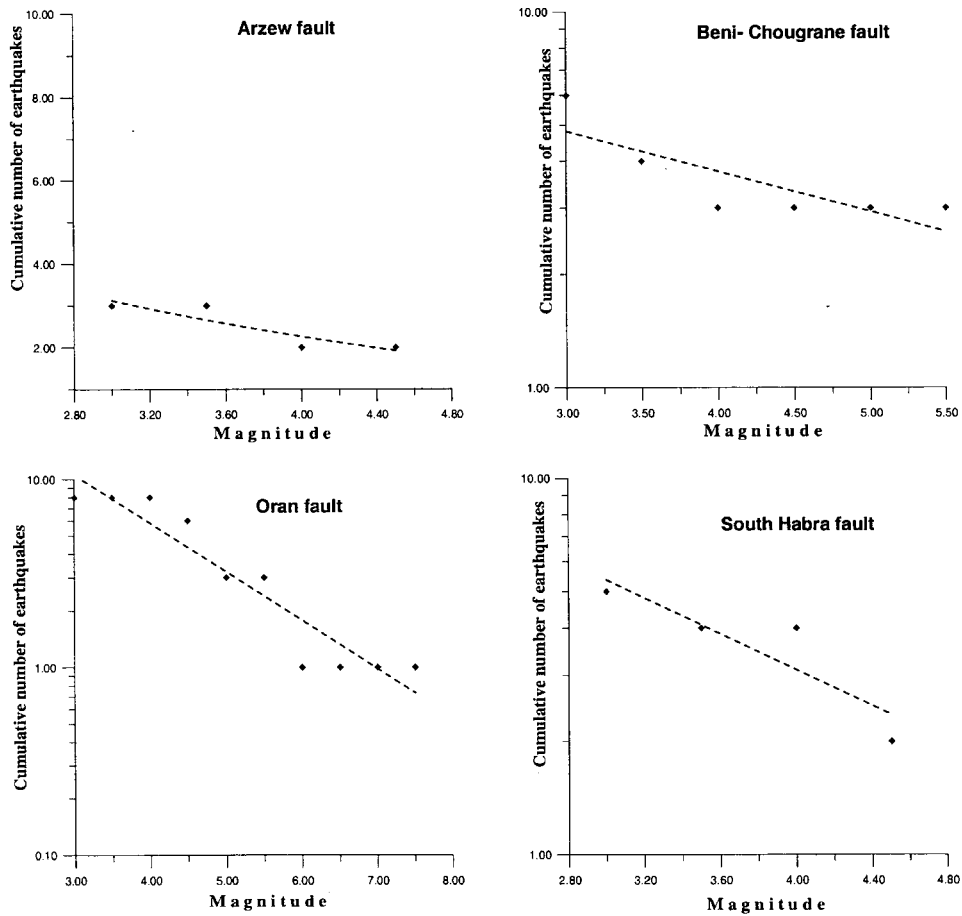


Figure 5. Plot of the cumulative number of earthquakes versus magnitude for some seismic sources of the studied area.

where  $m^1 = m^u - \Delta m^c$ , and  $\Delta m^c$  specifies the width of characteristic magnitude interval. The terms  $N^e$  and  $N^c$  represent the rate of exponential and characteristic events respectively.

## 5. Ground Motion Attenuation

One of the critical elements required in seismic hazard analysis is the attenuation relationship of peak ground acceleration (PGA). Ground motion attenuation relationships describe the variation of peak ground acceleration at specific structural periods of vibration and damping ratios with earthquake magnitude and source to site distance. Strong ground motions produced by earthquakes are influenced by the characteristics of the earthquake source, the crustal wave propagation path, and the local site geology. Accordingly, attenuation relationships typically are developed for specific tectonic environments. In this study, empirical attenuation relationships

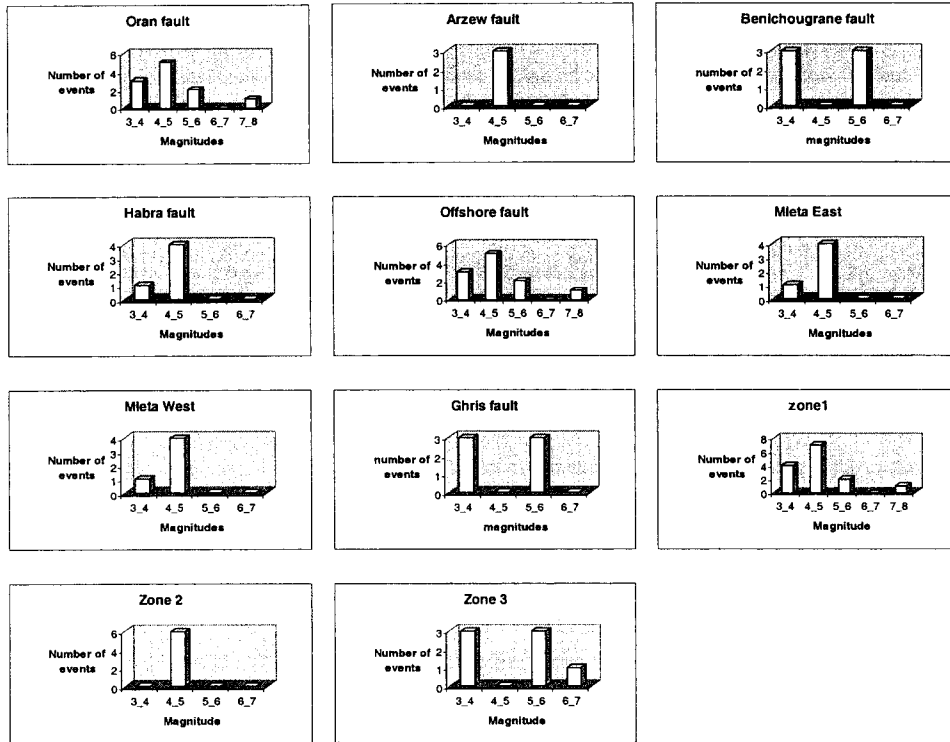


Figure 6. Histograms showing the distribution of earthquakes of various magnitudes for the defined seismic sources.

developed on the basis of statistical analysis of strong motion data recorded at locations having a similar tectonic environment were used. They are given by the following formulas of Sadigh *et al.* (1993):

$$\begin{aligned} \text{for } M \leq 6.5 : \ln(a_h) &= -0.624 + 1.0M - 2.10[\ln(R + \exp(1.29649 \\ &\quad + 0.25M))], \quad \sigma = 1.39 - 0.14M \\ \text{for } M > 6.5 : \ln(a_h) &= -1.274 + 1.1M - 2.10[\ln(R + \exp(-0.48451 \\ &\quad + 0.524M))], \quad \sigma = 0.38, \end{aligned} \quad (8)$$

where  $R$  is the closest distance to the rupture area,  $M$  is moment magnitude,  $a_h$  is maximum peak ground acceleration in ground surface, and  $\sigma$  is the standard error in  $\ln(a_h)$ .

Ambraseys and Bommer (1991) give:

$$\begin{aligned} \log(a_h) &= -0.338 + 0.238M_s - \log(r) - 0.00050r + 0.28P, \\ h &= 6.0 \text{ km}, \quad \sigma = 0.28, \end{aligned} \quad (9)$$

where  $r$  is the closest distance to the surface projection of the rupture surface,  $M_s$  is the surface magnitude and  $h$  is the depth,  $P$  ranges from 0 (for 50% percentile)

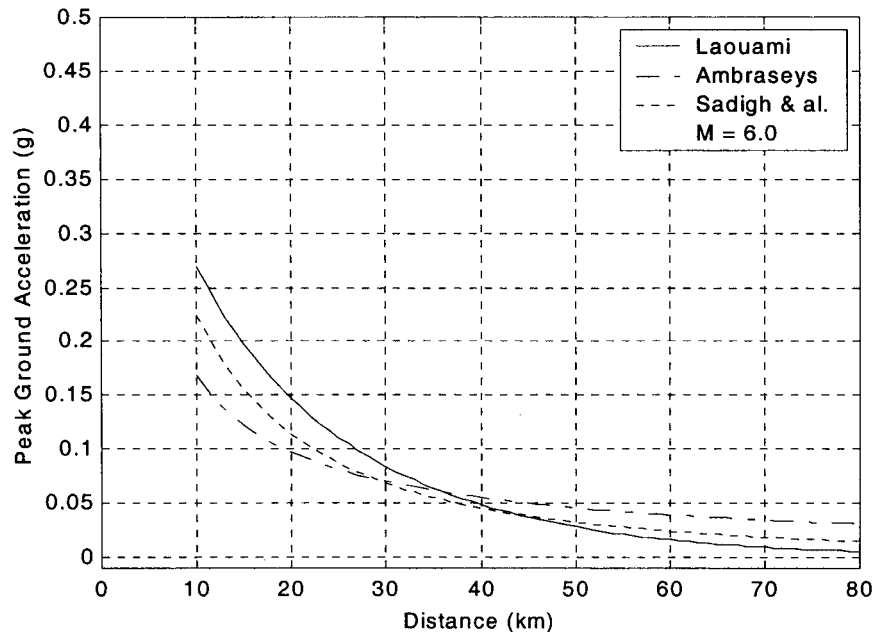


Figure 7. Comparison between the locally developed attenuation law (Laouami, 1998) and the Sadigh *et al.* (1993) and the Ambraseys and Bommer (1991) ones.

to 1 (for 84% percentile). Several studies (WCC, 1984; Laouami, 1998) show that these relationships fit Algerian data. Recently, based on a ground motion database recorded during the Beni Chougrane earthquake of August 18, 1994, Laouami (1998) derived a regional attenuation relationship which agrees well with Sadigh *et al.* (1993) and Ambraseys and Bommer (1991) relationships (Figure 7). Based on this result, the same weight (0.5) is attributed to relationships given by the Equations (8) and (9) for the computation of the seismic hazard of the studied region.

## 6. Results and Conclusion

Results of the seismic hazard assessment of the Oran region are presented herein as curves of relationships between values of peak ground acceleration and annual frequency of exceedance and relationships between these accelerations and return periods (Figure 8). Also, seismic hazard in terms of mean values of acceleration, is presented as zoning maps for return periods of 200 and 500 years (Figures 9 and 10) which are obtained by calculating hazard for different sites in a grid of 10 km  $\times$  10 km. Uncertainties due to the choices of parameters values and attenuation laws are presented as the mean, median (50% percentile), 15<sup>th</sup>, and 85<sup>th</sup> percentiles values of annual probability of exceedance.

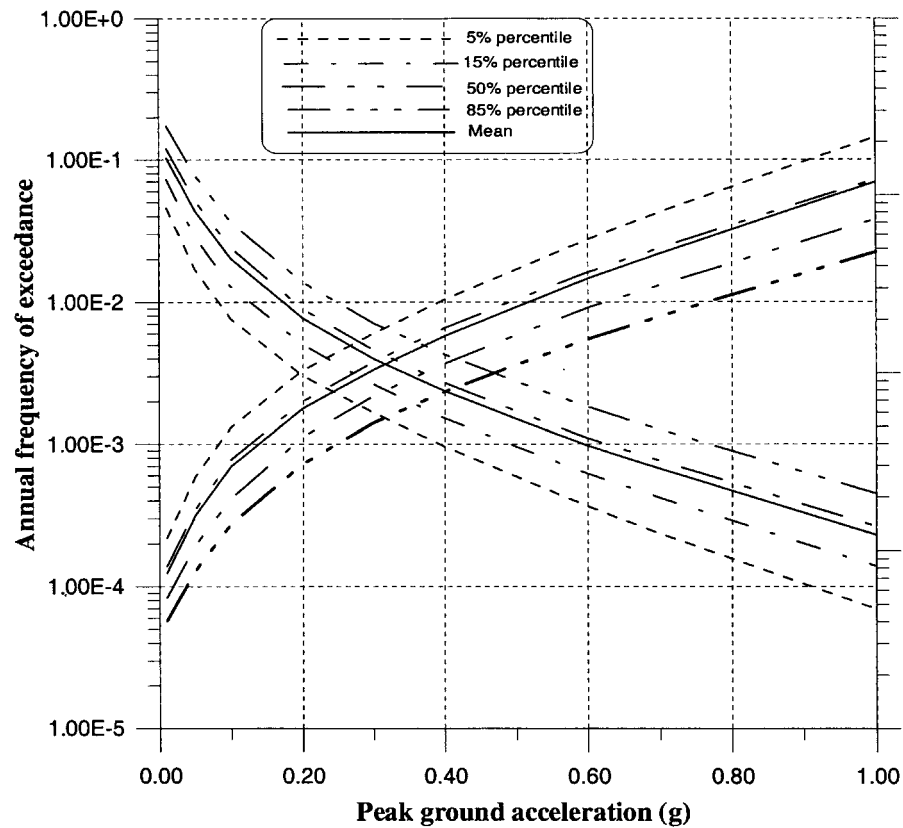


Figure 8. Plot of annual frequencies of exceedance and return periods versus peak ground accelerations for the Oran site ( $X = 0.624^\circ$  W,  $T = 35.660^\circ$  N).

Comparison between the two relationships (Ambraseys and Bommer, 1991 and Sadigh *et al.*, 1993) and the locally developed one (Figure 7) show that the Ambraseys and Bommer law (1991) underestimates the locally developed law up to the distance of 36 km, and overestimates it beyond; while the Sadigh *et al.* (1993) law underestimates the local one for short distances and agrees well for longer distances.

It appears from the obtained result (Figure 10) that seismic hazard in the studied region is dominated by the Oran fault, which is a major geological structure that likely produced the Oran earthquake of October 9, 1790 of intensity X. Indeed, high values of maximum peak ground acceleration in exceedance of 0.4 g are obtained in the vicinity of Oran site. Beside, recurrence of earthquakes on the geological structures, which are considered to be the primary cause of earthquakes, is taken into account through the characteristic model which considers the recurrence of strong earthquakes more important than that predicted by the exponential model based only on seismicity data. The obtained zoning maps should be a basic tool

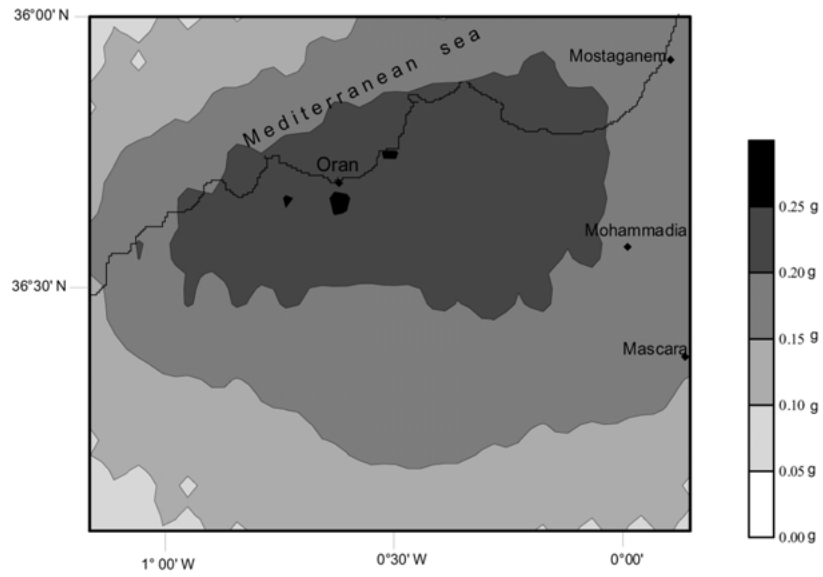


Figure 9. Seismic zoning map in terms of values of Peak Ground Accelerations of the Oran region, for a return period of 200 years.

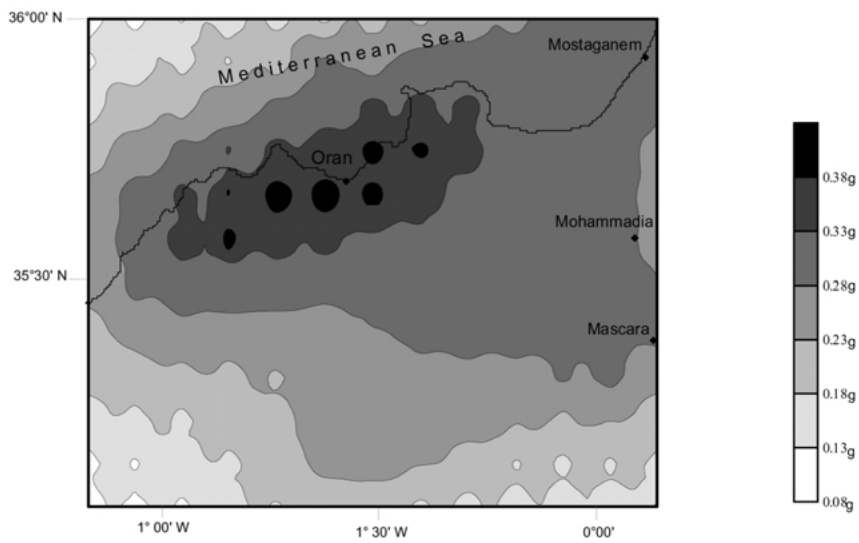


Figure 10. Seismic zoning map in terms of values of Peak Ground Accelerations of the Oran region, for a return period of 500 years.

for seismic risk mitigation and may serve for different purposes, particularly for administrators, planners and engineers.

The proposed seismic hazard assessment is based on the assumed seismic potential of geological structures which we believe, despite the lack of paleoseismic data, is sufficient to perform a reliable seismic hazard analysis. If we compare our results with the available studies in the region we remark that: (i) Using the deterministic approach by computation of complete synthetic seismograph by the modal summation approach, Aoudia *et al.* (2000) obtained values of 0.4–0.6 DGA (Design ground acceleration) for the Chelif zone including the studied region, hence, the results are comparable to ours. Indeed, Aoudia *et al.* (2000) pointed out the importance of the potential of geological structures in assessing seismic hazard. (ii) Seismic hazard maps presented by Jiménez *et al.* (1999), for the part of north of Algeria, seem to underestimate the seismic hazard because it's based on an incomplete catalogue of historical seismicity for the period of 1790–1975, updated by some data till 1989; The results are, hence, not different from those obtained by Morgat and Shah (1978). (iii) The Seismic hazard study performed by Benouar *et al.* (1996) is based on a compiled, completed and homogenised seismicity catalogue for the period of 1900–1990. We think, hence, that the results did not take into account effects of strong earthquakes of magnitude greater than 6.5 which are characterised by more long return periods (Meghraoui, 1988).

### Acknowledgement

The authors would like to thank four anonymous reviewers for their valuable comments.

### References

- Ambraseys, N. N. and Bommer, J. J.: 1991, The attenuation of ground accelerations in Europe, *Earthquake Eng. Struct. Dyn.* **20**, 1179–1202.
- Aoudia, A. and Meghraoui, M.: 1995, Seismotectonics in the Tell Atlas of Algeria: The Tenes-Abou-El hassan earthquake of 25/08/1922  $M = 6.0$ , *Tectonophysics* **248**, 263–276.
- Aoudia, A., Vaccari, F., Suhadolc, P., and Meghraoui, M.: 2000, Seismogenic potential and earthquake hazard assessment in the Tell Atlas of Algeria, *Journal of Seismology* **4**, 79–98.
- Benouar, D.: 1994, The seismicity of Algeria and adjacent regions, *Annali di geofisica* **37**, 459–862.
- Benouar, D., Aoudia, A., Maouche, S., and Meghraoui, M.: 1994, The August 18, 1994 Mascara earthquake – A quick look report, *Terra-nova* **6**, 634–637.
- Benouar, D., Molas, G. L., and Yamazaki, F.: 1996, Earthquake hazard mapping in the Maghreb countries, *Earthq. Eng. & Struct. Dyn.* **25**, 1151–1164.
- Bezzeghoud, M. and Bufforn, E.: 1999, Source parameters of the 1992 Melilla (Spain,  $M_w = 4.8$ ), 1994 Alhoceima (Morocco,  $M_w = 5.8$ ), 1994 and Mascara (Algeria,  $M_w = 5.7$ ) earthquakes and seismotectonics implications', *Bull. Seismol. Soc. Am.* **89**(2), 359–372.
- Bouhadad, Y.: 1997, Tectonique active et aléa sismique dans le bassin de Chelif occidental, *Proceedings. Etat de l'art et perspectives en prévention sismique*, IGC-USTO et CRAAG, 32 pp.
- CGS (Centre National de Recherche Appliquée en Génie Parasismique): 1995, The Benichougrane earthquake of August 18, 1994. Preliminary technical report, CGS, 40 pp.

- Cornell, C. A.: 1968, Engineering seismic risk analysis, *Bull. Seismol. Soc. Am.* **58**, 1583–1606.
- Cornell, C. A. and Van Marke, E. H.: 1969, The major influence on seismic risk, *Proceedings of the Third Conference on Earthquake Engineering*, Vol. A-1, Santiago, Chile, pp. 69–93.
- CRAAG (Centre de Recherche en Astronomie Astrophysique et Géophysique): 1994, Les séismes de l'Algérie de 1365 ... 1992, Publication du CRAAG, Alger, 227 pp.
- De Mets, C. R., Gordon, R. G., Argus, D. F., and Stein, S.: 1990, Current plate motions, *Geophys. J. Inter.* **101**, 425–478.
- El Ghobrini, M.: 1986, *Evolution morphostructurale de la marge algérienne occidentale (Méditerranée occidentale): Influence de la néotectonique et de la sédimentation*, Thèse doct., University of Sorbonne, France, 164 pp.
- Geomatrix Consultants: 1993, Probabilistic seismic hazard analysis computer program: A user manual.
- Gutenberg, B. and Richter, C. F.: 1954, *Seismicity of the Earth and Associated Phenomena*, Princeton University Press, NJ, 310 pp.
- Jiménez, M. J., Garcia-Fernandez, and the GSHAP Ibero-Maghreb Working Group: 1999, Seismic hazard assessment in the Ibero-Maghreb Region, *Annali di Geofisica* **42**, 1057–1066.
- Kijko, A. and Sellevoll, M. A.: 1989, Estimation of earthquake hazard parameters from incomplete data files. Part II. Incorporation of magnitude heterogeneity, *Bull. Seismol. Soc. Am.* **82**(1), 120–134.
- Laouami, N.: 1998, Etude expérimentale sur l'atténuation du mouvement sismique. Elaboration de lois d'atténuation empiriques pour les régions de l'Algérie du Nord. Rapport interne CGS, 55 pp.
- McGuire, R. K.: 1976, FRISK: Computer program for seismic risk analysis using faults as earthquake sources, *U.S. Geological Survey*. Open file report 78-1007.
- McGuire, R. K.: 1993, Computations of seismic hazard, *Annali di geofisica* **XXXVI**(3–4), 181–200.
- McKenzie, D. P.: 1972, Active tectonics of the Mediterranean region, *Geophys. J. Resear.* **30**, 109–185.
- Meghraoui, M.: 1988, *Géologie des zones sismiques du Nord de l'Algérie. Paléosismologie, tectonique active et synthèse sismotectonique*, Thèse Doct., University Paris Sud France, 356 pp.
- Meghraoui, M.: 1990, Blind reverse faulting system associated with the Mont Chenoua-Tipaza earthquake of 29 October 1989 (North central Algeria), *Terra nova* **3**, 84–93.
- Meghraoui, M., Philip, H., Albarede, F., and Cisternas, S. A.: 1988, Trench investigations through the trace of the 1980 El Asnam thrust fault: Evidence for paleoseismology, *Bull. Seismol. Soc. Am.* **78**(2), 979–999.
- Meghraoui, M., Morel, J. L., Andrieux, J., and Dahmani, M.: 1996, Tectonique plio-quadernaire de la chaîne tello-rifaine et de la mer d'Alboran. Une zone complexe de convergence continent-continent, *Bull. Soc., Géol. France* t.**167**(1), 141–157.
- Merritts, D. and Bull, W. B.: 1989, Quaternary uplift rates at the Mendocino triple junction, Northern California from uplifted marine terraces, *Geology* **17**, 1020–1024.
- Morgat, C. and Shah, H. C.: 1978, Seismic hazard analysis of Algeria, Report J. A. Blume Earthq. Eng. Center, Stanford University.
- NRC (National Research Council): 1988, *Probabilistic Seismic Hazard Analysis*, National Academy Press, Washington, D.C. 96 pp.
- Philip, H. and Thomas, G.: 1977, Détermination de la direction de raccourcissement de la phase de compression quaternaire en Oranie (Algérie), *Revue de Géographie Phys. Géol. Dynam.* **XIX**, fasc.4, 315–324.
- Philip, H. and Meghraoui, M.: 1983, Structural analysis and interpretation of the surface deformation of the El Asnam earthquake of October 1980, *Tectonics* **2**, 17–49.
- Philip, H.: 1987, Plioquaternary evolution of the stress field in Mediterranean zones of subduction and collision', *Ann. Geophys.* **5B**, 301–320.
- Sadigh, K., Chang, C. Y., Abrahamson, N. A., Chiou, S. J., and Power, M. S.: 1993, Specification of long period ground motion. Updated attenuation relationships for rock site conditions and



- adjustment factors for near fault effects, *Proceedings of ATC-17-1 Seminar on Seismic Isolation, Passive Energy Dissipation, and Active Control, 11–12 March*, San Francisco, CA, pp. 59–70.
- Swan, F. H.: 1988, Temporal clustering of paleoseismic events on the Oued Fodda fault, Algeria, *Geology* **16**, 1092–1095.
- Thomas, G.: 1985, *Géodynamique d'un bassin intramontagneux. Le bassin de Chellif occidental (Algérie) durant le mio-plio-quaternaire*, Thèse. Doct., University de Pau et pays de l'Addour, France, 548 pp.
- Toro, G. R.: 1995, Probabilistic seismic hazard analysis: A review of the state of the art, *Proceedings of the 5th Intern. Conf. Seis. Zon., 17–19 October, 1995*, Nice-France, III, pp. 1829–1856.
- Wells, D. L. and Coppersmith, K. J.: 1994, Updated empirical relationships among magnitude, rupture length, rupture area, and surface displacement, *Bull. Seismol. Soc. Am.* **84**, 974–1002.
- WCC (Woodward Clyde Consultants): 1984, Seismic microzonation of Ech-Chellif region, Algeria. Report prepared for C.T.C., Algiers, 1, CTC, Algeria, 145 pp.
- Yielding, G, Ouyed, M., King, G. C. P., and Hazfeld, D.: 1989, Active tectonics of the Algeria Atlas mountains. Evidence from aftershocks of the 1980 El-Asnam earthquake. *Geophy. J. Inter.* **99**, 761–788.
- Youngs, R. R. and Coppersmith, K. J.: 1985, Implication of fault slip rates and earthquakes recurrence models to probabilistic seismic hazard estimates, *Bull. Seismol. Soc. Am.* **75**, 939–964.

